

THE RADIAL VELOCITY FIELD OF THE OPTICAL FILAMENTS ASSOCIATED WITH THE SNR W63

M. Rosado and J. González

Instituto de Astronomía
Universidad Nacional Autónoma de México

Received 1980 May 13

RESUMEN

Se presenta el campo de velocidades radiales de filamentos ópticos pertenecientes al remanente de supernova W63. Se obtienen velocidades de expansión para este remanente de $35 \pm 12 \text{ km s}^{-1}$ o de $70 \pm 30 \text{ km s}^{-1}$, según se considere que el cascarón óptico corresponde a la radiofuente no-térmica W63 ($< 1^\circ$) o bien se identifique con todo el complejo de filamentos que aparecen en las placas de Palomar ($\sim 4^\circ$). Para ambos casos se calcula el cociente E_0/n_0 y se dan límites superiores para la densidad pre-choque. Estos valores se comparan con aquellos derivados a partir de los datos espectroscópicos existentes.

ABSTRACT

We obtained the radial velocity field of some optical filaments of the SNR W63. We estimated for its expansion velocity values of $35 \pm 12 \text{ km s}^{-1}$ and $70 \pm 30 \text{ km s}^{-1}$ depending on whether the SNR is thought to be the non-thermal radio source W63 ($< 1^\circ$) or the whole filamentary complex shown on Palomar Plates ($\sim 4^\circ$). We derived the SNR ratio E_0/n_0 for both cases and we found upper limits for the pre-shock density. We compared those with the values derived from the available spectroscopic data.

Key words: INTERFEROMETRY – NEBULAE – SUPERNOVA REMNANTS – RADIAL VELOCITIES.

I. INTRODUCTION

The fairly extended radio source W63 (G82.2 + 5.4) located in the NW part of the Cygnus X region, has been identified as a SNR by many authors (Aizu and Tavera 1967; Ilovaisky and Lequeux 1972; Clark and Caswell 1976; Wendker 1971) on the basis of its steeper spectral index ($\alpha \approx -0.7$) and its high degree of linear polarization (Velusamy and Kundu 1974). We believe that W63 qualifies as SNR.

Table 1 gives a summary of the main radio properties of W63. From the Σ -D relationship we derived a mean distance of 1.6 kpc, in good agreement with the distance of most filamentary structures in the Cygnus X region as derived from their optical reddening (Dickel, Wendker and Bieritz 1969). However, (Wendker 1971), the latter method places the same filaments at a somewhat larger value, beyond 2 kpc.

On the PSS prints, W63 appears associated with a much larger complex of filamentary nebulae, centered at $\alpha(1950) = 20^h 21^m 04^s$, $\delta(1950) = 44^\circ 22'$, and with an angular diameter of 220 arcmin. Such an association is strongly supported by the following arguments:

a) The high [S II]/H α ratio of the complex appears similar to that of W63. This result comes from interference-filter photographs, (Parker, Gull and Kirshner 1979) two of them reproduced in Plate 2 (Figure 1) and spectroscopic data (Lozinskaya *et al.* 1976).

b) There are enhancements at 2695 MHz near the optical filaments (Wendker 1971). Furthermore, the Haslam *et al.* (1974) global radio continuum survey shows W63 at the edge of a much greater ring.

Nevertheless, we shall analyze below the data for both possibilities: a small object of 77 arcmin diameter or a full 220 arcmin ring.

TABLE 1

PROPERTIES OF W63 DERIVED FROM RADIO DATA

θ ($'$ arc)	ν	$\Sigma_{\nu}(\text{W m}^{-2} \text{ Hz}^{-1}$ $\text{strd}^{-1})$	α	Distance (kpc)	Diameter (pc)	Ref.
77.6	1 GHz	0.32 (– 20)	1.4	32.6	(1)
77	408 MHz	0.642(– 20)	– 0.7	{ 1.7	{ 37.6	(2)
				{ 1.8	{ 39.8	(3)
68	400 MHz	0.36 (– 20)	– 0.3	1.9	38.4	(4)
77	1 GHz	0.38 (– 20)	– 0.7	{ 1.6	{ 35.9	(5)
				{ 1.3	{ 28.6	(6)

(1) Ilovaisky and Lequeux (1972).

(2) Clark and Caswell (1976).

(3) Caswell and Lerche (1979). Taking into account the z -dependence on the $\Sigma - D$ relation.

(4) Downes (1971).

(5) Milne (1979).

(6) Milne (1979). Taking into account the z -dependence.

II. THE OBSERVATIONS

The observations of two regions of the brightest nebulosities of W63 were carried out with a focal reducer at the Cassegrain focus of the 83 cm reflector of the Observatorio Astronómico Nacional, B.C.N. The obtained material consisted of three $\text{H}\alpha$ -photographs taken with a narrow band interference filter (λ 6563 Å, $\Delta\lambda = 10$ Å) and two Fabry-Pérot interferograms covering the regions previously photographed. Two of the $\text{H}\alpha$ -photographs are reproduced in Figure 2 (Plate 3). On Figure 3 we show the location of the fields of the interferograms within the whole nebula. The measurements of the interferograms were performed on the Vibrating Mirror comparator of the Marseille Observatory. The reductions were made in the standard way (Courtès 1960).

III. THE RADIAL VELOCITY FIELD AND ITS IMPLICATIONS

Figures 4 and 5 show the radial velocity field of W63 obtained from the interferograms covering the fields marked in Figure 3. The measurements are in good agreement with Lozinskaya's data. The reported velocities relative to the Sun were corrected for solar motion and galactic rotation. Assuming that W63 is at a distance of 1.6 kpc, the galactic rotation effect amounts only to $+4 \text{ km s}^{-1}$. This value is in agreement with the velocity obtained by taking an overall mean of the points in the interferograms; this turns out to be of $-3 \pm 8 \text{ km s}^{-1}$. Although there is no direct evidence of an expansion, such as a splitting of the interference rings, it is quite likely that an expansion is taking place because of the thin shell appearance. With this assumption an ellipse can be traced in the $r\text{-}V_r$

plane, as described in Rosado *et al.* (1980) in order to derive the most likely expansion velocity.

In this case some complications arise: a) If we assume that the true shape of W63 is that obtained from radio observations, we realize that this shape differs from the simple spherical case. In fact, we have an ellipsoid with major and minor axes of 105 and 60 arcmin respectively. Then, r would be the distance from the projection of the observed point on the plane perpendicular to the line of sight to the center of the ellipsoid. This elliptical shape can be due to inhomogeneities in the density of the preshock material. In spite of the non-spherical shape shown by the radio isophotes, we decided to study the kinematics in the simple, spherical-shell case. This is justified by the fact that we have measured only the radial velocities of the brightest filaments and their shape can be approximated by a spherical shell having a radius equal to the major axis of the ellipsoid. Thus, assuming a spherical geometry for the brightest filaments, we obtain a semi-ellipse in the $r\text{-}V_r$ plane (see Figure 6). This ellipse has the property of having major and minor axes equal to the maximum radius of the nebula and to the expansion velocity, respectively (as described in Rosado *et al.* 1980). From these assumptions, we obtain an expansion velocity of $35 \pm 12 \text{ km s}^{-1}$. We also find that some other points, identified with nebulosities ahead of the shell, are localized in regions of the $r\text{-}V_r$ plane, external to that of the ellipse. Thus, presumably they belong to a foreground nebulosity.

b) As we have already discussed in Section 1 we can also assume that W63 is part of a spherical complex with an angular diameter of 220 arcmin. For this case we can trace the ellipse in an easier way, since now the maximum radius must be the radius of

the spherical shell. In this manner, we obtain an expansion velocity of $70 \pm 30 \text{ km s}^{-1}$ as Figure 7 shows.

IV. DISCUSSION

We have thus derived two values for the expansion

velocity of W63, namely $35 \pm 12 \text{ km s}^{-1}$ assuming a radio size of 77 arcmin in angular diameter (Case *a*), or $70 \pm 30 \text{ km s}^{-1}$ assuming the apparent optical size of 220 arcmin in angular diameter (Case *b*). For a distance of 1.6 kpc, we can obtain the shock radius, R_s , and the shock velocity, V_s . In order to obtain this last

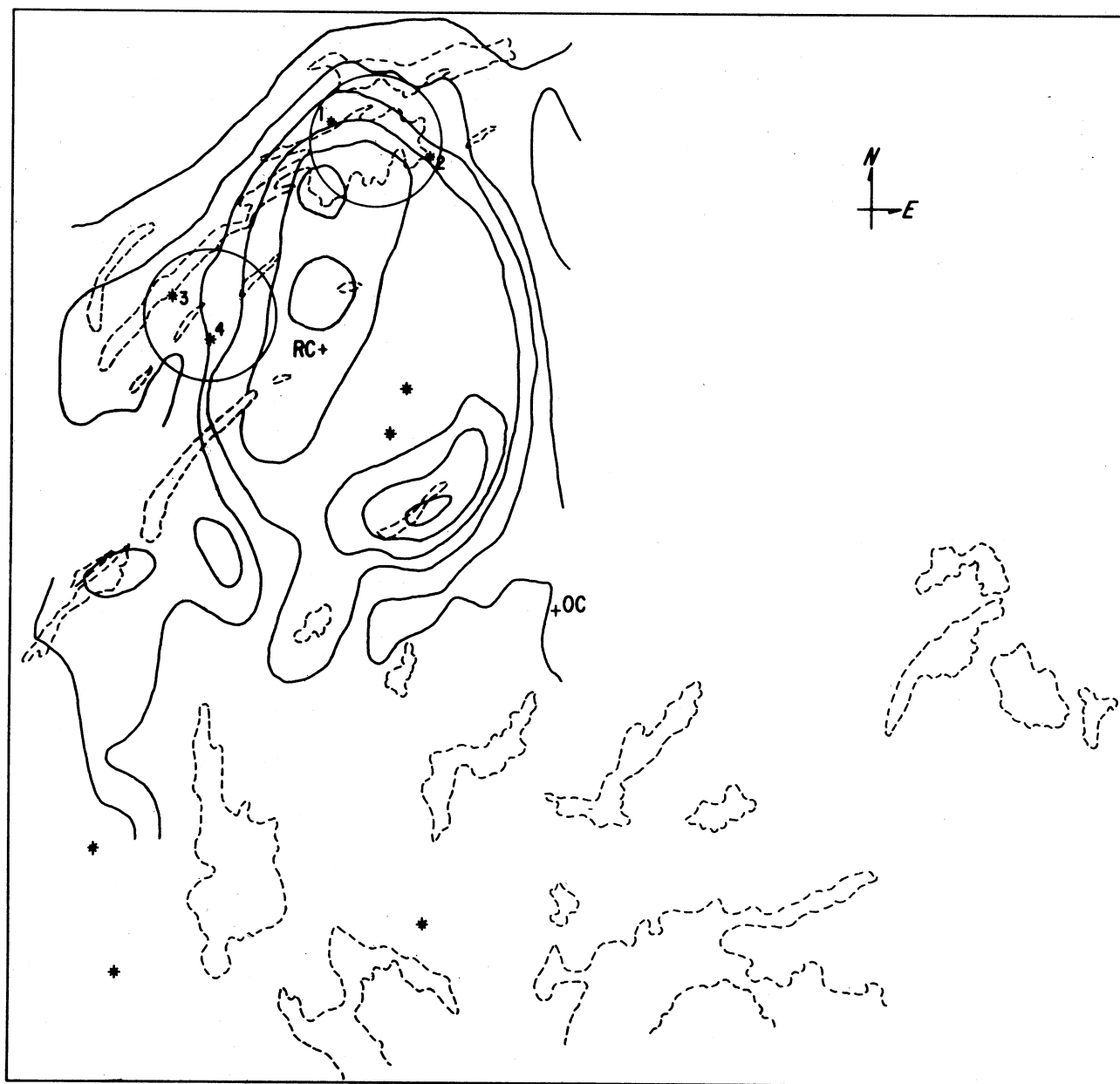


Fig. 3. Location of the fields of the interferograms in the whole nebula (solid circles). Solid lines represent radio isophotes of W63 (Wendker 1971); dashed lines represent the optical nebulosities. Stars 1, 2, 3 and 4 are the reference stars shown in the radial velocity field (Figures 4 and 5) and the crosses represent the optical (OC) and the radio (RC) centers, respectively.

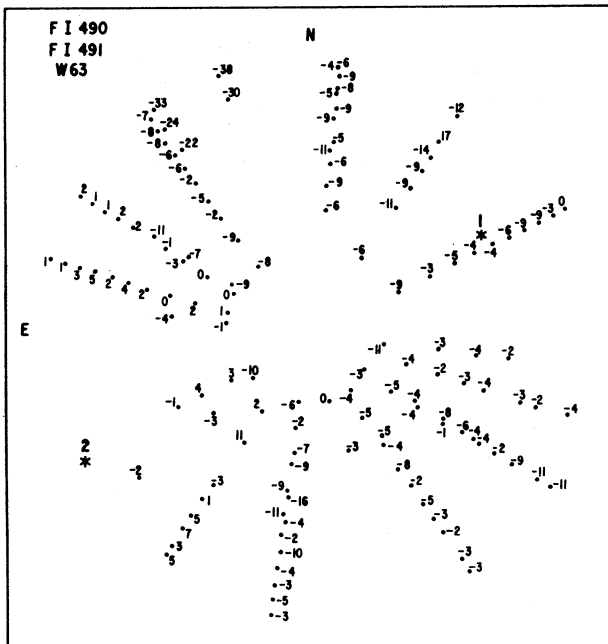


Fig. 4. The radial velocity field derived from two interferograms of the filaments of W63 shown in Plate 2.

quantity we assume the shock to be isothermal, in which case the expansion velocity will be the same as the shock velocity. We think this to be always the case since what one measures optically is a velocity coming

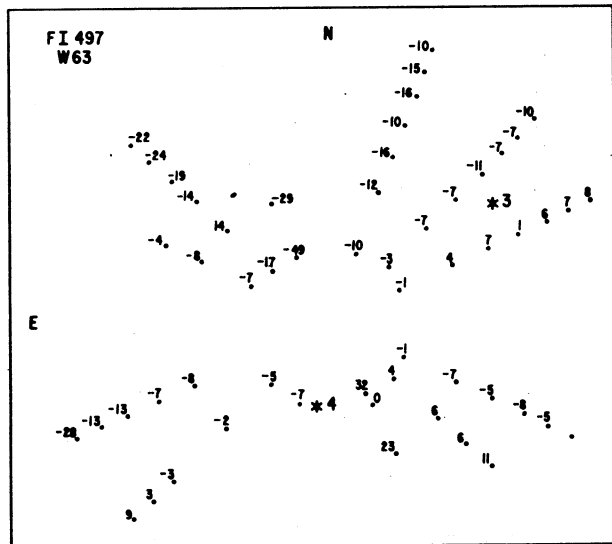


Fig. 5. The radial velocity field, derived from one interferogram of the filaments of W63 shown in Plate 2.

from the gas located in the recombination zone of the shock and in this zone the shock is isothermal. Then, we have for Case *a*

$$\begin{cases} R_s = 18 \text{ pc,} \\ V_s = 35 \text{ km s}^{-1}, \end{cases}$$

and for Case *b*

$$\begin{cases} R_s = 53 \text{ pc,} \\ V_s = 70 \text{ km s}^{-1}. \end{cases}$$

We checked the validity of these values by comparing them with those derived from the application of theoretical shock models to the spectroscopic observations of Lozinskaya (1974) and to the estimated value of the line-ratio $[O \text{ III}]/(H\alpha + [N \text{ II}])$ derived from the photographs of Parker *et al.* (1979). Table 2 gives the observed line-ratios together with the models that agree best with observations (Raymond 1979; Shull and McKee 1979). From this table, we see that either Raymond's model AA or Shull and McKee's model D could explain the observed values within the observational uncertainties. These models correspond to quite different shock conditions: Model AA refers to a shock of 60 km s^{-1} moving in a pre-ionized medium of $n_0 = 350 \text{ cm}^{-3}$ of pre-shock density while Model D corresponds to a shock of 90 km s^{-1} in a medium with $n_0 = 10 \text{ cm}^{-3}$. The latter model assumes that there are no pre-ionizing sources and the ionization state is obtained in a self-consistent way. Thus, from the spectroscopic observations we cannot discriminate between the kinematical value of the expansion velocities obtained assuming Case *a* or *b*, since we can have either a relatively fast shock supplying the observed $[S \text{ II}]/H\alpha$ line-ratio by itself or a slow shock with additional sources of pre-ionization that could explain this line-ratio. On the other hand, in Case *b* the observed $[S \text{ II}]$ electron densities and the expansion velocity can be used in principle to derive the pre-shock density. Taking the $[S \text{ II}]$ 6717/6731 line ratio (Lozinskaya *et al.* 1976), we obtain $n_e \sim 800\text{--}4000 \text{ cm}^{-3}$, which gives $n_0 \sim 40\text{--}200 \text{ cm}^{-3}$, not too different from that of Model D (10 cm^{-3}). Then, in a general way, we see that the values of the pre-shock density, obtained by either one of the two assumptions (Case *a* or *b*) are relatively high, but also highly uncertain. From the kinematical values for the shock velocity already obtained, we can derive some relations between the ratio of energy of the SN explosion to the pre-shock density, E_0/n_0 , depending on whether W63 is in the adiabatic phase of its evolution or in the radiative phase. In order to do that we take the relations given by Cox (1972) for the adiabatic phase and by Chevalier (1974) for the radiative phase.

If we assume that Case *a* holds, then

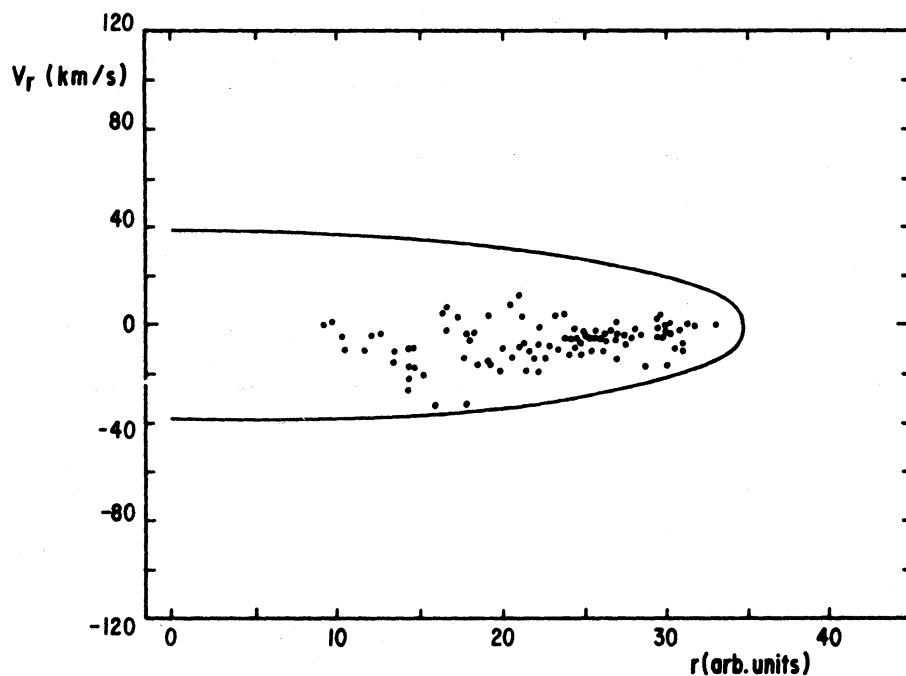


Fig. 6. Fitted ellipse to the radial velocities versus radii data for Case *a*, discussed in the text.

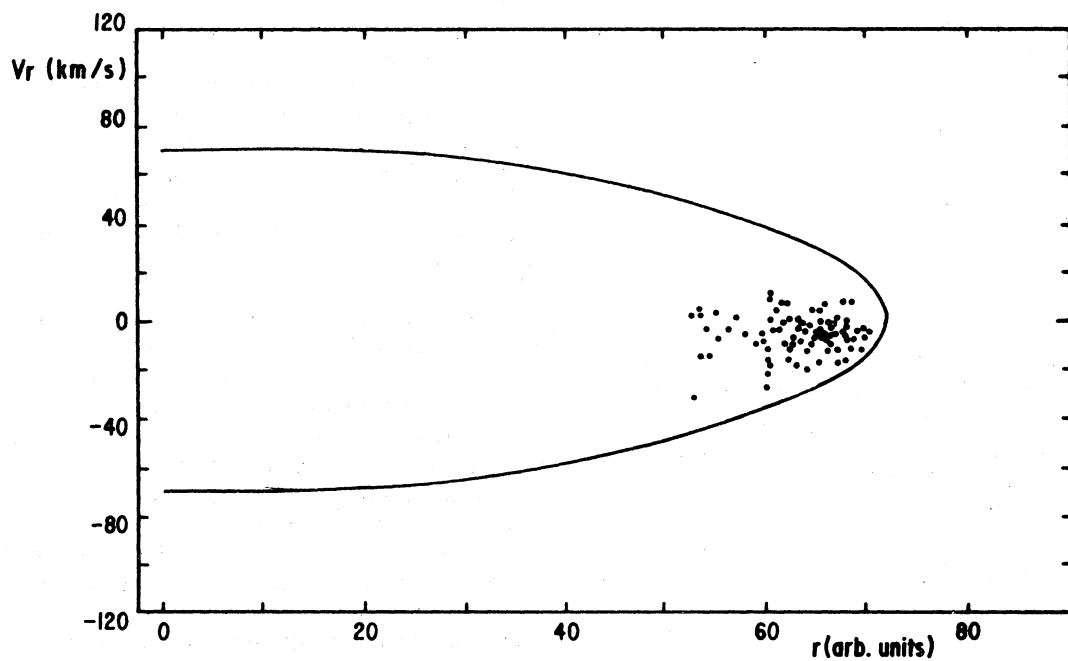


Fig. 7. Same as for Figure 6, for Case *b*.

TABLE 2
COMPARISON OF THE SPECTROSCOPIC DATA WITH SHOCK MODELS

Line Ratios	Observed Values	Ref.	Predictions by Models	
			Raymond (1979) Model AA	Shull and McKee (1979) Model D
[N II] ($\lambda\lambda 6548 + 6584$)/H α	0.68 ± 0.13	(1)	1.01	0.82
[S II] ($\lambda\lambda 6717 + 6731$)/H α	0.6 ± 0.1	(1)	0.38	0.82
[S II] $\lambda\lambda \left(\frac{6717}{6731} \right)$	0.8 ± 0.2	(1)	0.73	1.22
[O III] ($\lambda\lambda 4959 + 5007$) H α + [N II] ($\lambda\lambda 6548 + 6584$)	$\lesssim 0.3$	(2)	0.27	0.34

(1) Lozinskaya *et al.* (1976).
(2) Parker *et al.* (1979).

$$\left. \frac{E_0}{n_0} \right|_{AD} = 9.8 \times 10^{48}$$

or

$$\left. \frac{E_0}{n_0^{1.12}} \right|_{RA} = 6.3 \times 10^{49}$$

while for Case *b*, we obtain

$$\left. \frac{E_0}{n_0} \right|_{AD} = 1.0 \times 10^{51}$$

or

$$\left. \frac{E_0}{n_0^{1.12}} \right|_{RA} = 4.9 \times 10^{51}$$

where E_0 is given in ergs and n_0 in cm^{-3} .

The relations given above, impose an upper limit to the pre-shock density in order to have energies of the SN explosion of the same order of magnitude as those found in classical SNR, i. e., E_0 limited to the range 10^{50} to 10^{52} ergs. Taking the upper limit of $E_0 = 10^{52}$ ergs for Case *a* to hold,

$$n_{0AD} \lesssim 1020 \text{ cm}^{-3}, \text{ or}$$

$$n_{0RA} \lesssim 92 \text{ cm}^{-3}.$$

While for Case *b* we obtain

$$n_{0AD} \lesssim 10 \text{ cm}^{-3} \text{ or}$$

$$n_{0RA} \lesssim 2 \text{ cm}^{-3}.$$

The latter results seem to favor lower values for the pre-shock density if Case *b* holds. Thus, these energetic considerations tend to place the pre-shock density of W63 at values much lower than those deduced from the observed line-ratios. However, these ratios are quite uncertain specially on the low density side, and further discussion must await more accurate measurements of the line-ratios.

In conclusion, in order to discriminate between the two possibilities assumed above, namely that the linear diameter deduced from the radio observations is correct (Case *a*), and consequently we have a shock of 35 km s^{-1} , or that the SNR has an angular shape greater than that derived from the radio observations (Case *b*), implying a shock of 70 km s^{-1} , we suggest that further observations and reductions be made as follows:

1) More accurate spectroscopy of the filaments should be obtained in order to have better values of the line-ratios. From these the large range allowed for the electron densities would be reduced.

2) Measurements of the photographic densities of the narrowband interference-filter plates should be performed, in order to have a bi-dimensional picture of the structure of the filaments.

3) Deep X-ray observations will help greatly to discriminate between the fast and slow shock hypotheses and to derive the true size of the SNR.

The authors are greatly indebted to Dr. A. Laval for her help in the measurements and to A. Campa for his assistance during the observations.

REFERENCES

- Aizu K. and Tavera, H. 1967, *Progress of Theo. Phys.*, 37, 296.
 Caswell, J.L. and Lerche, I. 1979, *M.N.R.A.S.*, 187, 201.
 Chevalier, R.A. 1974, *Ap. J.*, (Paper I), 188, 501.
 Clark, D.H. and Caswell, J.L. 1976, *M.N.R.A.S.*, 174, 267.
 Cox, D.P. 1972, *Ap J.*, 178, 159.
 Courtès, G. 1960, *Ann. D'Ap.*, 23, 115
 Dickel, H.R., Wendker, H., Bieritz, J.H. 1979, *Astr. and Ap.*, 1, 270.
 Downes, D. 1971, *A.J.*, 76, 305.
 Haslam, C.G.T., Wilson, W.E., Graham, D.A., and Hunt, G.C. 1974, *Astr. and Ap. Suppl.*, 13, 359.
 Ilovaisky, S.A. and Lequeux, J. 1972, *Astr. and Ap.*, 18, 169.
 Lozinskaya, T.A., Klement'eva, A. Yu., Zhukov, G.V., and Shenavrin, V.I. 1976, *Sov. Astron.*, 19, 416.
 Milne, D.K. 1979, *Austr. J. Phys.*, 32, 83.
 Parker, A.R., Gull, T.R., Kirshner, R.P. 1979, in *An Emission-Line Survey of the Milky Way*, NASA SP-434, (Washington, D.C.: NASA).
 Raymond, J.C. 1979, *Ap. J. Suppl.*, 39, 1.
 Rosado, M., Georgelin, Y., Laval, A., Monnet, G. 1978, to appear in *Astr. and Ap.*
 Shull, J.M. and McKee, C.F. 1979, *Ap. J.*, 227, 131.
 Velusamy, T. and Kundu, M.R. 1974, *Astr. and Ap.*, 32, 375.
 Wendker, H.J. 1971, *Astr. and Ap.*, 13, 65.

Javier González and Margarita Rosado: Instituto de Astronomía, UNAM, Apdo. Postal 70-264, México 20, D.F., México

